Supplementary Information (SI) Appendix

Identification of a negative-strand RNA virus with natural plant and fungal hosts

Ruoyin Dai[a], Shian Yang[a], Tianxing Pang[a], Mengyuan Tian[a], Hao Wang[a], Dong Zhang[b], Yunfeng Wu[a], Hideki Kondo[c], Ida Bagus Andika*[d], Zhensheng Kang[a], Liying Sun*[a,c,e]

[a] State Key Laboratory of Crop Stress Resistance and High-Efficiency Production and College of Plant Protection, Northwest A&F University, Yangling 712100, China

[b] Yangling Sub-Center of National Center for Apple Improvement and College of Horticulture, Northwest A&F University, Yangling 712100, China

[c] Institute of Plant Science and Resources, Okayama University, Kurashiki 710-0046, Japan

[d] College of Plant Health and Medicine, Qingdao Agricultural University, Qingdao 266109, China

[e] Institute of Future Agriculture, Northwest A&F University, Yangling 712100, China

Includes:

SI Figures, Figure S1-S10

SI Tables, Table S1 and S2

SI Materials and methods

A

Number of tissue samples and *V. mali* strains from the field orchards

Sampling location		No. tissue samples	No. fungal isolates
Yangling District		8	58
Xunyi County	1	39	217
	2	8	49
	3	27	90
Wugong County	1	9	94
	2	11	53
Qian County	1	12	52
	2	31	209
Liquan County	1	16	221
	2	3	31
	3	2	31
Total		167	1110

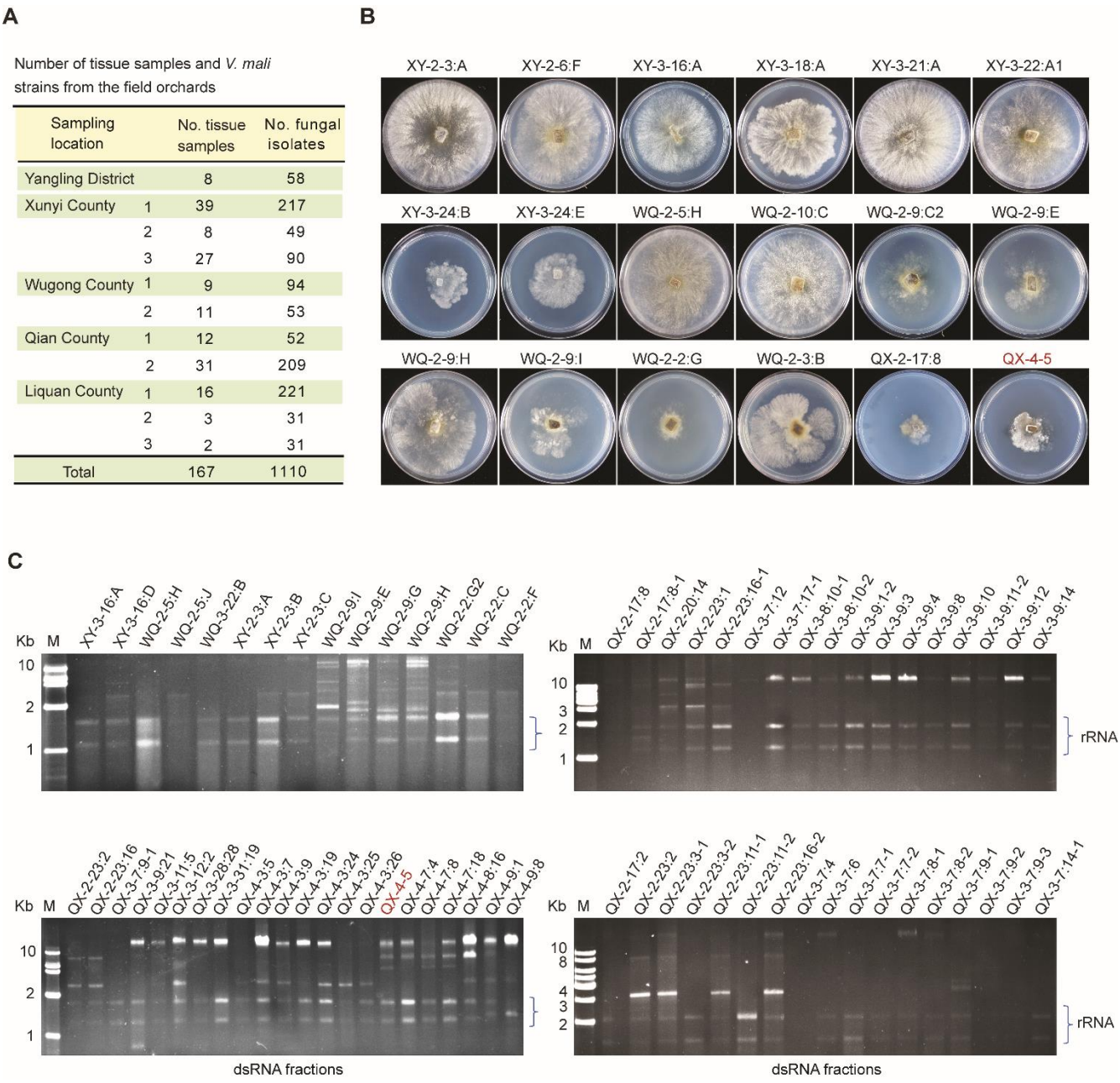

Figure S1. Isolation of *V. mali* strains from apple trees grown in orchards in the Shaanxi Province of China. (A) Number of tissue samples and *V. mali* fungal strains collected from each sampling site. (B) Phenotypic growth of representative *V. mali* strains on PDA medium. The fungi were photographed at 5 days after culturing. (C) Representative agarose gel electrophoresis images of dsRNA fractions extracted from *V. mali* strains. M represents a DNA size marker.

A

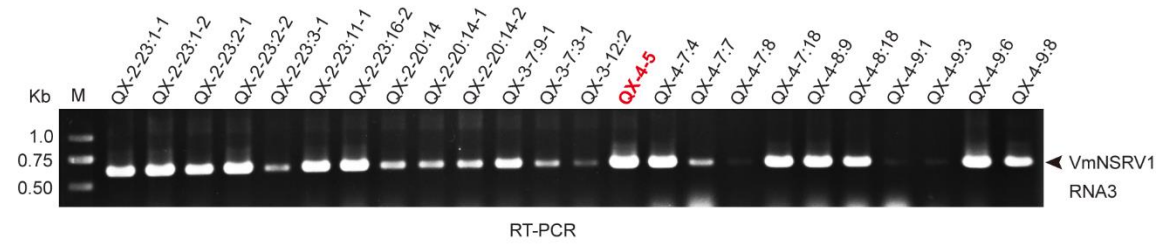

RT-PCR

B

Detection of VmNSRV1 in *V. mali* strains isolated from the fields

Samppling area	dsRNA-containing fungi	dsRNA-free fungi
Yangling District	1/1	1/2
Xunyi County	10/10	3/5
Wugong County	8/11	1/1
Qian County	12/26	0/7
Liquan County	35/43	2/4
Total	66/91 (72.5%)	7/19 (36.4%)

Number of virus-infected isolates/Number of tested isolates

Figure S2. **Detection of VmNSRV1 in *V. mali* strains.** (A) Representative agarose gel electrophoresis images of the RT-PCR detection of VmNSRV1 RNA3 accumulation in *V. mali* strains. (B) Number of *V. mali* strains (dsRNA-containing or dsRNA-free fungal strains) with VmNSRV1 infection as detected by RT-PCR. M represents a DNA size marker.

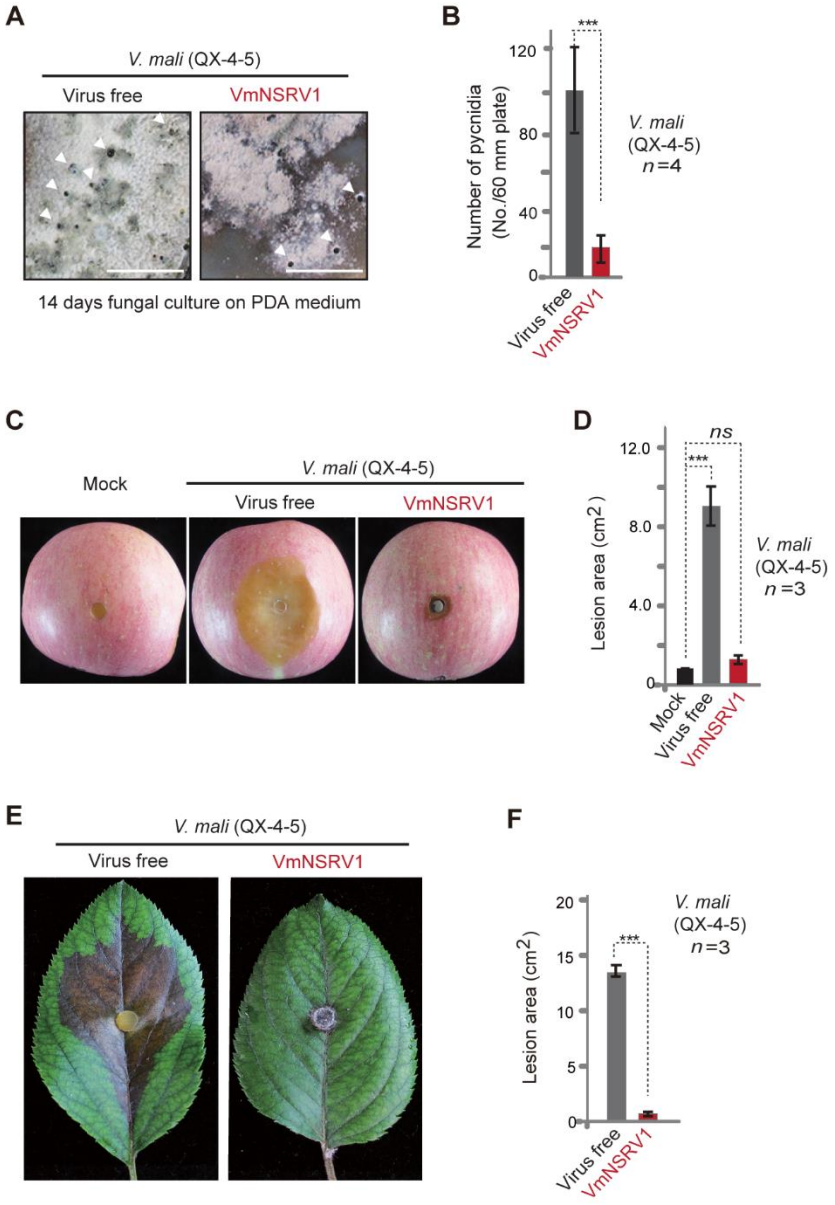

Figure S3. **Effects of VmNSRV1 infection on *V. mali*.** (A) Photographs showing the formation of pycnidia in virus-free and VmNSRV1-infected *V. mali* (QX-4-5) culture on PDA medium. Arrowheads mark the pycnidia. Scale bars, 1 cm. (B) Number of mature pycnidia formed in *V. mali* culture. "***" indicates significant differences ($P < 0.001$, Student's *t*-test). (C) Virulence assay of a *V. mali* (QX-4-5) strain on apple fruits. Fungal lesions were photographed at 5 days after inoculation. (D) Measurement of fungal lesions observed in the experiment described in (C). "***" indicates significant differences ($P < 0.001$, Student's *t*-test), and "*ns*" indicates a non-significant difference. (E) Virulence assay of a *V. mali* (QX-4-5) strain on apple leaves. Fungal lesions were photographed at 5 days after inoculation. (F) Measurement of fungal lesions observed in the experiment described in (E). "***" indicates significant differences ($P < 0.001$, Student's *t*-test).

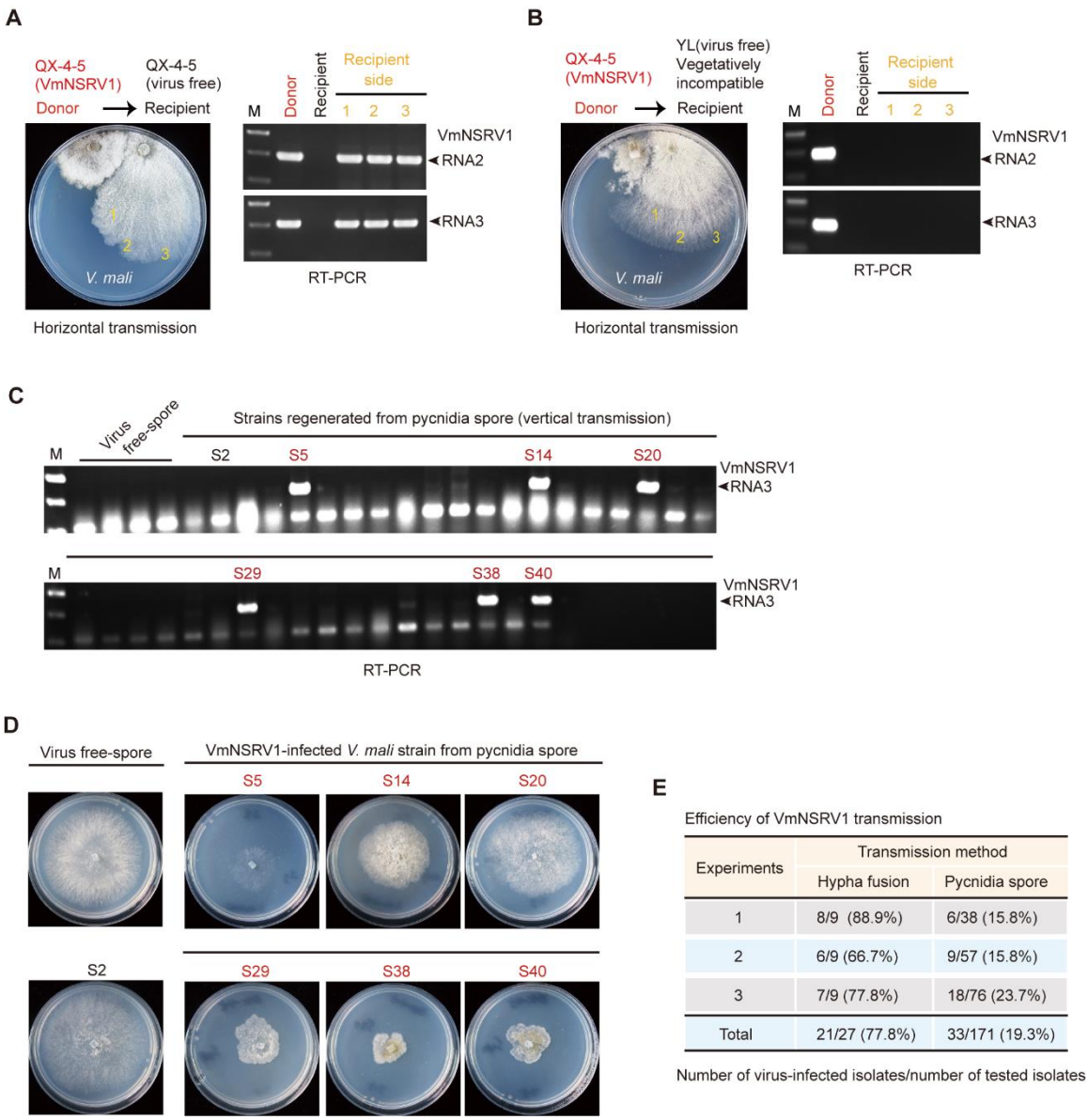

Experiments	Transmission method	
	Hypha fusion	Pycnidia spore
1	8/9 (88.9%)	6/38 (15.8%)
2	6/9 (66.7%)	9/57 (15.8%)
3	7/9 (77.8%)	18/76 (23.7%)
Total	21/27 (77.8%)	33/171 (19.3%)

Figure S4. **Horizontal and vertical transmission of VmNSRV1 infection in *V. mali*.** (A) Co-culturing of two isogenic strains of virus-free and VmNSRV1-infected *V. mali* QX-4-5 (as a vegetatively compatible combination) to assess VmNSRV1 transmission through hyphal fusion. The fungi were photographed at 5 days after culturing. Fungal strains were obtained from the recipient side of the fungus and VmNSRV1 infection was detected by RT-PCR using RNA2 and RNA3 specific primer sets. (B) Co-culturing of two vegetatively incompatible strains of *V. mali* (QX-4-5 and YL). VmNSRV1 RNA2 and RNA3 were detected by RT-PCR in the recipient fungal side. (C) Representative agarose gel electrophoresis images of the RT-PCR detection of VmNSRV1 in *V. mali* (QX-4-5) strains regenerated from spores produced by *V. mali* pycnidia infected with VmNSRV1. (D) Phenotypic growth of representative virus-free and VmNSRV1-infected *V. mali* (QX-4-5) strains described in (C**)**. (E) Transmission efficiency of VmNSRV1 through hyphal fusion and pycnidium as assessed by RT-PCR using RNA3 specific primers. M represents a DNA size marker.

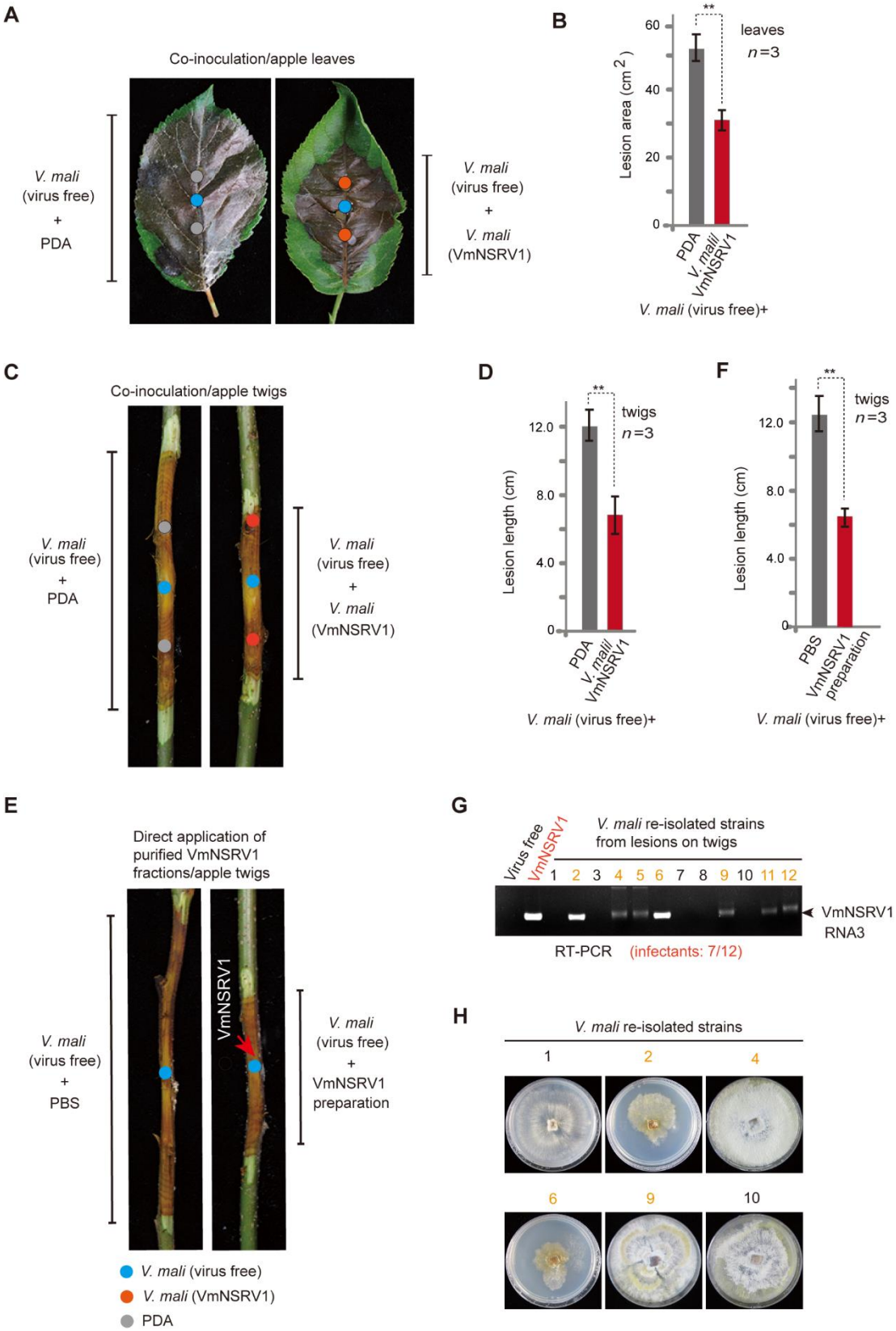

Figure S5. Suppression of *V. mali* pathogenicity by VmNSRV1 transmission through hyphal fusion or direct application of purified VmNSRV1. (A) Co-inoculation of virus-free and VmNSRV1-infected *V. mali* (QX-4-5) strains on apple leaves. (B) Fungal lesion areas measured from the experiment described

in (A). "**" indicates significant differences ($P < 0.01$, Student's *t*-test). (C) Co-inoculation of virus-free and VmNSRV1-infected *V. mali* (QX-4-5) strains on apple twigs. (D) Fungal lesion lengths measured in the experiment described in (C). "**" indicates significant differences ($P < 0.01$, Student's *t*-test). (E) Direct application of purified VmNSRV1 to *V. mali* mycelia (virus-free QX-4-5 strain) inoculated on apple twigs. (F) Fungal lesion lengths measured from the experiment described in (E). "**" indicates significant differences ($P < 0.01$, Student's *t*-test). (G) RT-PCR detection of VmNSRV1 RNA3 in *V. mali* strains re-isolated from lesions on apple twigs described in (E). (H) Phenotypic growth of representative re-isolated *V. mali* strains with VmNSRV1 infection or without virus infection. The fungi were photographed at 5 days after culturing. Fungal lesions were photographed at 10 days after inoculation in (A), (C), and (E).

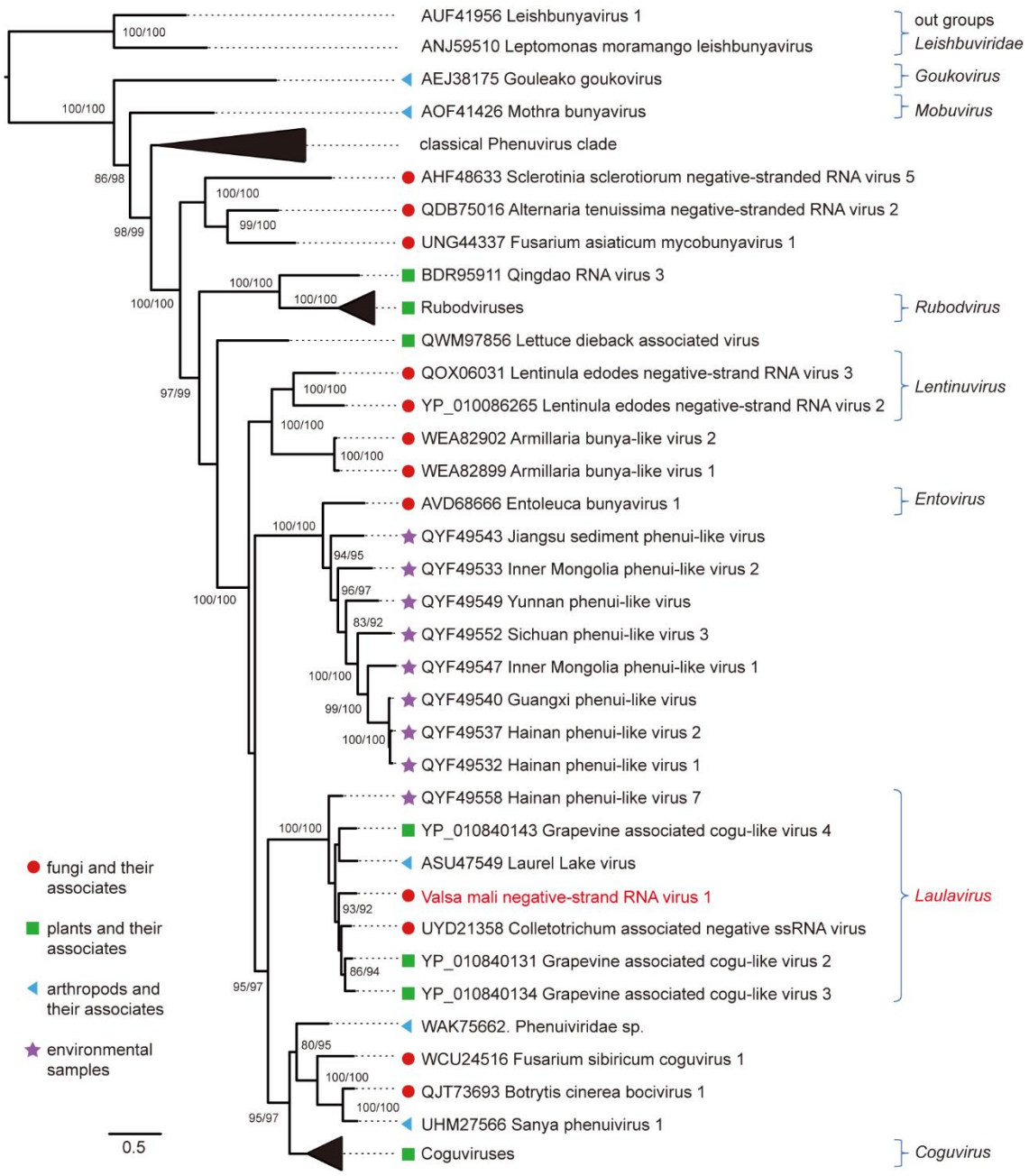

Figure S6. **Phylogenetic relationships of VmNSRV1 with phenuiviruses or other selected phenui-like viruses.** The maximum likelihood tree was based on multiple sequence alignment of the RNA1-encoded protein L (RdRp). The virus names are preceded by their accession numbers. The two distantly related RNA viruses outside the phenuivirus lineage (*Leishbuviridae*) were used as outgroups. The scale bar represents amino acid distances. Branch numbers indicate SH-aLRT support (%)/ultrafast bootstrap support (%); only values >80% are shown. Some clades were collapsed into a triangle. The classical phenuivirus clade consists of Severe fever with thrombocytopenia syndrome virus (*Bandavirus*, AMT85885), Badu virus (*Phasivirus*, AMA19446), Rift Valley fever phlebovirus (*Phlebovirus*, YP_003848704), Rice stripe virus RNA 1 (*Tenuivirus*, NP_620522), Hubei diptera virus 3 (*Beidivirus*, APG79285), Wuhan horsefly virus (*Horwuvirus*, AJG39260), Hubei diptera virus 4 (*Hudivirus*, APG79298), Pidgey bunyavirus (*Pidchovirus*, AOX47534), and Hubei lepidoptera virus 1 (*Hudovirus*,

APG79261). The Rubodvirus clade consists of Apple rubbery wood virus 1 (AWC67511), Apple rubbery wood virus 2 (AWC67530), Grapevine Muscat rose virus (EM04319), and Grapevine Garan dmak virus (YP_010840095). The Coguvirus clade consists of Citrus concave gum-associated virus 1 (AST13127), Citrus virus A (AYN78568), Citrus leaf flecking-associated virus (QBZ68778), Watermelon crinkle leaf-associated virus 1 (ASY01340), Watermelon crinkle leaf-associated virus 2 (ASY01343), Blackberry line pattern virus (WDD63192), Brassica campestris chinensis coguvirus 1 (YP_0108408), Edgeworthia chrysantha mosaic-associated virus (UZA34087), and Yunnan Paris negative-stranded virus (YP_010840810).

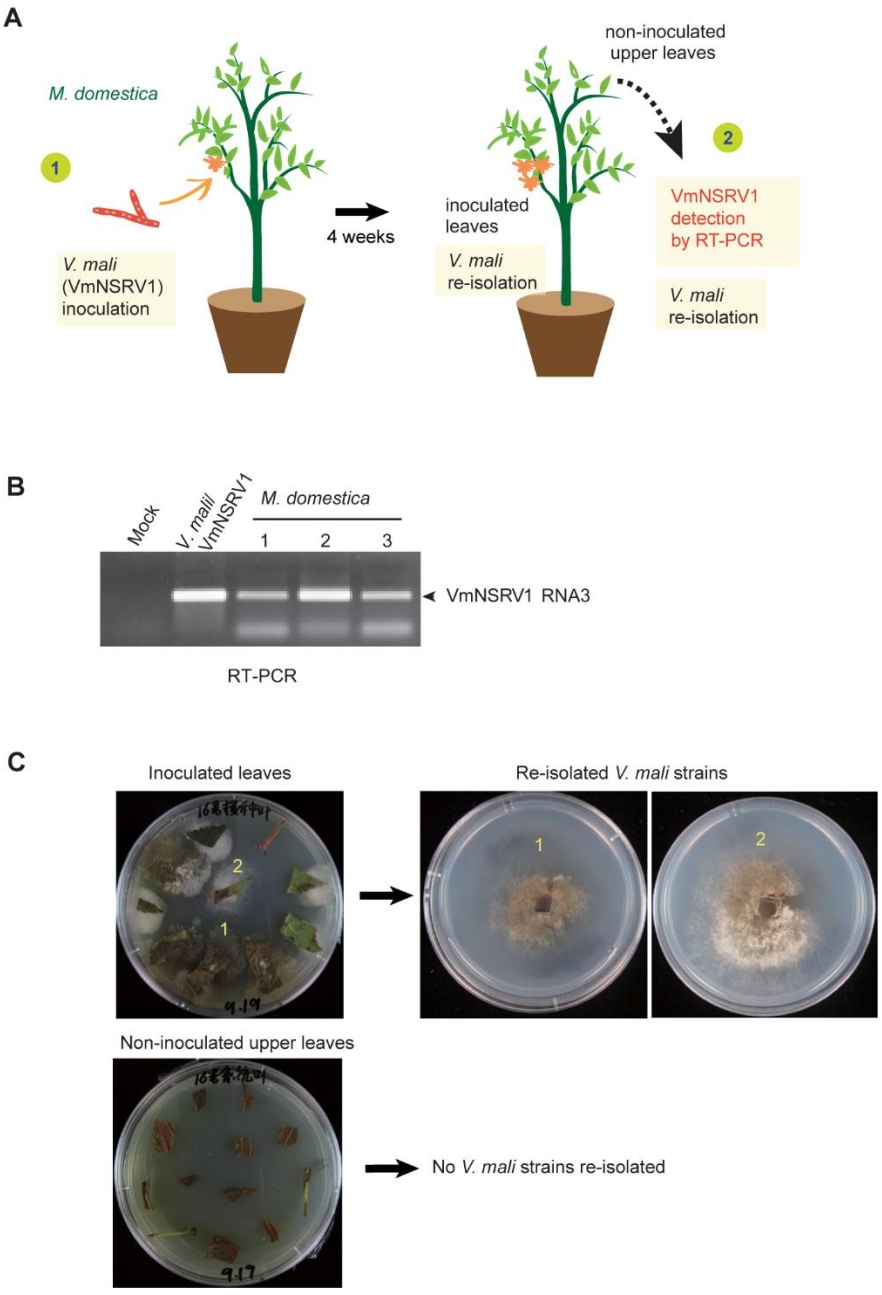

Figure S7. **VmNSRV1 transmission from fungus to plant.** (A) An illustration showing the experimental procedure used to investigate the transmission of VmNSRV1 from *V. mali* to the apple plant (*M. domestica*). (1) Inoculation of leaves with mycelia of a VmNSRV1-infected *V. mali* (QX-4-5) strain. (2) RT-PCR detection of VmNSRV1 in non-inoculated upper leaves 4 weeks after fungal inoculation. (B) Agarose gel electrophoresis image of the RT-PCR detection of VmNSRV1 RNA3 in non-inoculated upper leaves from the experiment described in (A**)**. (C) Leaf tissue from fungus-inoculated leaves and non-inoculated upper leaves was placed on PDA medium to assess the presence of *V. mali* strains in the tissue. *V. mali* grew on fungal-inoculated leaves but did not on non-inoculated upper leaves. The fungi were photographed at 5 days after culturing.

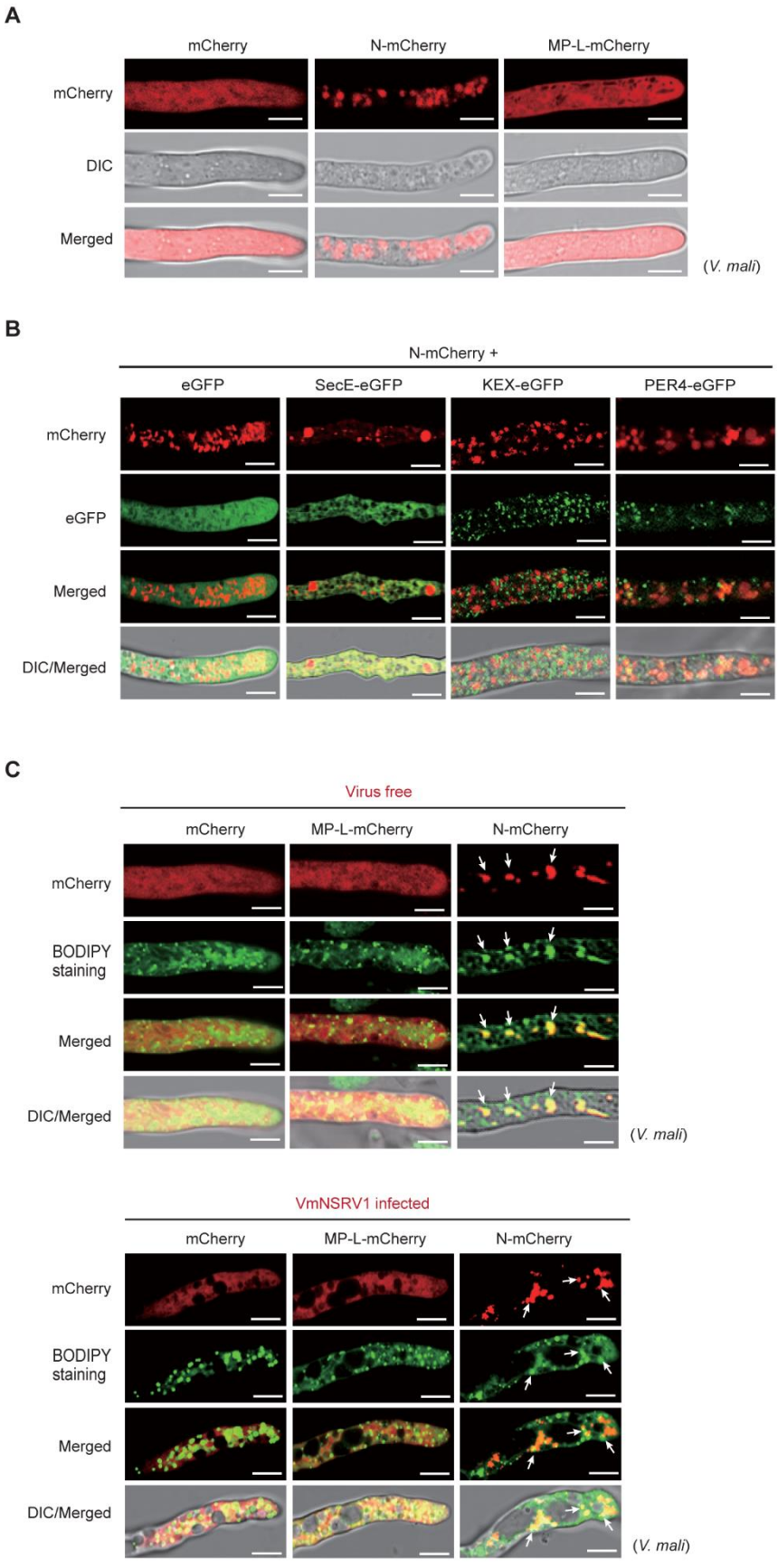
A
mCherry
N-mCherry
MP-L-mCherry
mCherry
DIC
Merged
(V. mali)
B
N-mCherry +
eGFP
SecE-eGFP
KEX-eGFP
PER4-eGFP
mCherry
eGFP
Merged
DIC/Merged
(V. mali)
C
Virus free
mCherry
MP-L-mCherry
N-mCherry
mCherry
BODIPY staining
Merged
DIC/Merged
(V. mali)
VmNSRV1 infected
mCherry
MP-L-mCherry
N-mCherry
mCherry
BODIPY staining
Merged
DIC/Merged
(V. mali)

Figure S8. **Subcellular localization of the VmNSRV1 MP-L and N proteins in *V. mali*.** (A) Expression of N or MP-L protein fused to mCherry (N-mCherry or MP-L-mCherry) in a virus free *V. mali* (QX-4-5) strain. Fluorescence in mycelial cells was observed using CLSM. Scale bars, 10 μm. (B) Co-expression of N-mCherry with eGFP, endoplasmic reticulum (SecE-eGFP), trans-Golgi network (KEX-eGFP), and peroxisome (PER4-eGFP) markers in a virus free *V. mali* (QX-4-5) strain. Scale bars, 10 μm. (C) Treatment of virus-free and VmNSRV1-infected fungi (QX-4-5) expressing MP-L-mCherry or N-mCherry with BODIPY 493/503 to stain lipid droplets. Arrows indicate the representative overlapping fluorescence signals. Scale bars, 10 μm.

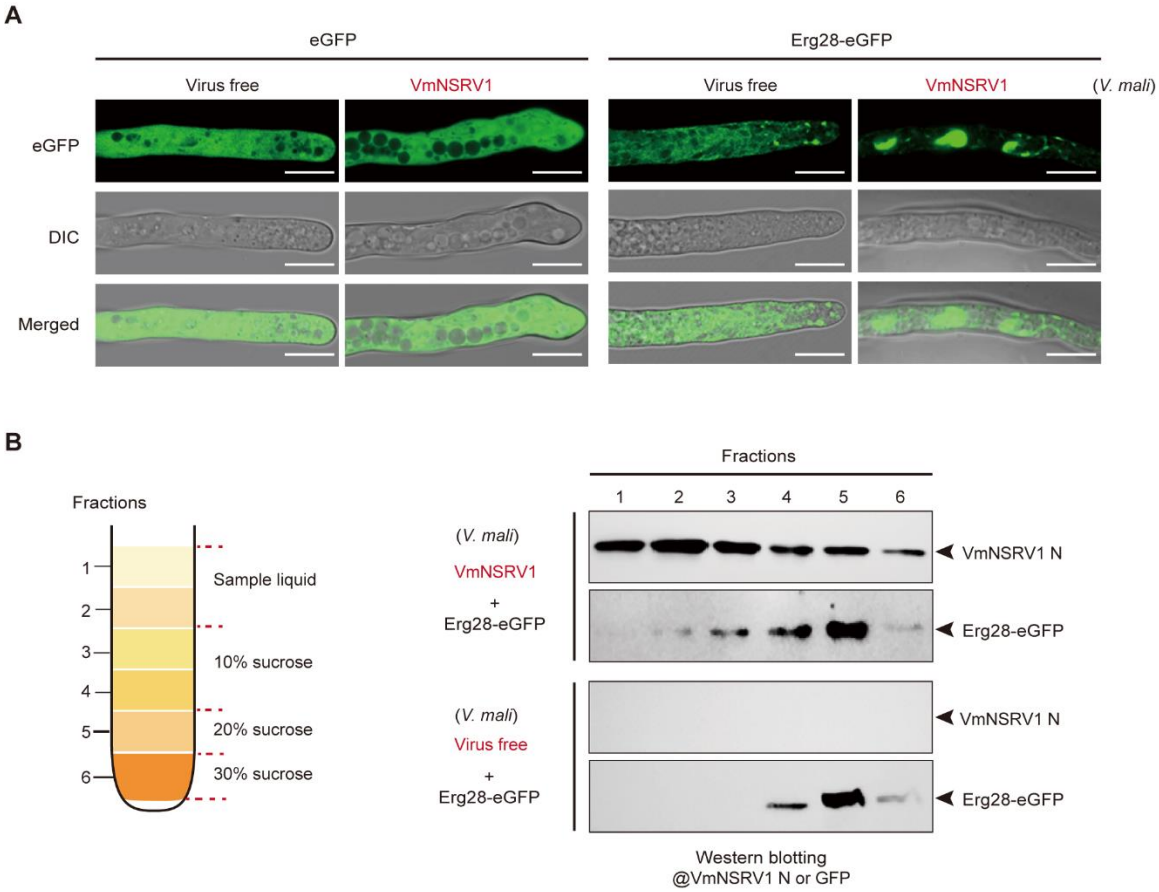

Figure S9. **Effects of VmNSRV1 infection on lipid droplet structure.** (A) Subcellular localization of Erg28-eGFP (lipid droplet marker) in virus-free and VmNSRV1-infected *V. mali* (QX-4-5) strains. Fluorescence in mycelial cells was observed using CLSM. Scale bars, 10 μm. (B) Fractionation of total extracts of virus-free and VmNSRV1-infected *V. mali* (QX-4-5) mycelia by sucrose density gradient ultracentrifugation (left panel) and immunoblot detection of Erg28-eGFP and the VmNSRV1 N protein in the fractions to examine the velocity sedimentation of lipid droplets (right panel). Immunoblotting was performed using antibodies specific for the GFP (to detect Erg28-eGFP) and VmNSRV1 N protein, respectively.

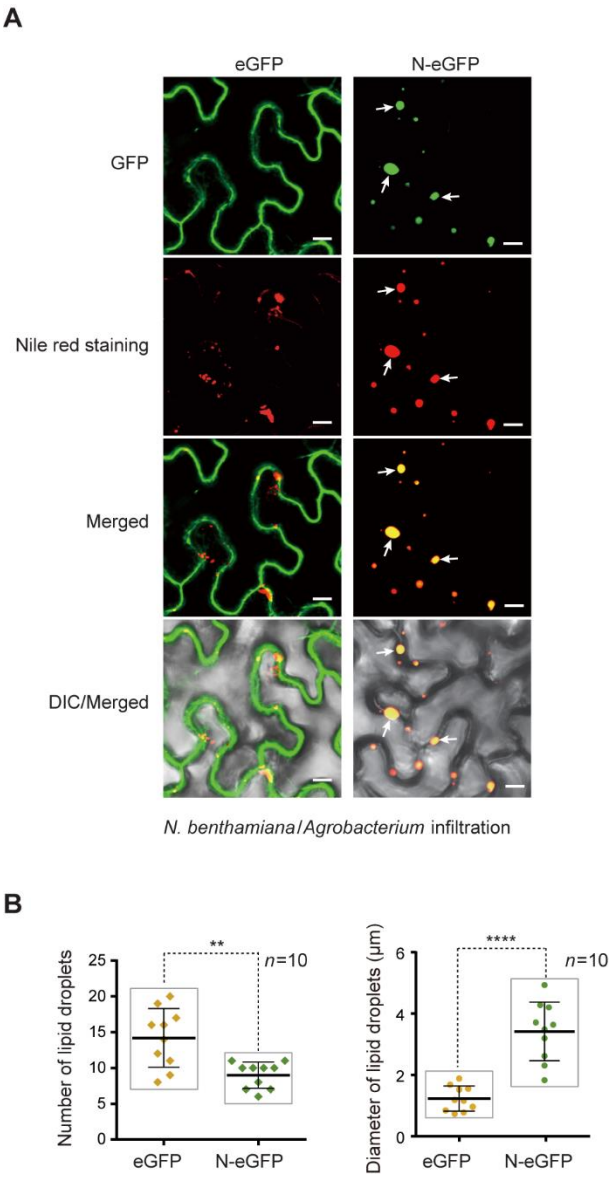

Figure S10. **Association of VmNSRV1 N protein with lipid droplets in plant cells.** (A) Subcellular localization of N protein fused to eGFP (N-eGFP) in the epidermal cells of *N. benthamiana* plants transiently expressed by *Agrobacterium* infiltration. The cells were treated with Nile red staining to visualize lipid droplets. Fluorescence was observed by CLSM 3 days after *Agrobacterium* infiltration. Arrows indicate the representative overlapping fluorescence signals. Scale bars, 10 μm. (B) Quantification and measurement of the number and size of lipid droplets observed in the staining experiment described in (A). "**" or "****" indicates significant differences (P <0.01 or 0.0001, Student's t-test).

Table S1. A list of primers used in this study.

Clone Name	Primer Name	Oligonucleotide sequence (5'- 3')
Primers used for VmNSRV1 full-length sequence		
RNA1 5′ and 3′ RACE	L-3' RACE	CTCCTGAAGAGAAGGATGAGGTGTCTC
	L-5' RACE	GAGGTTAGTGCATCTCTCCTGGTGC
RNA2 5′ and 3′ RACE	M-3' RACE	CAAAGGAAGAATATGTGAGGAGGCAAG
	M-5' RACE	CAAGAGTGTCAACCATGTCATCATCG
RNA3 5′ and 3′ RACE	S-3' RACE	GGAACTAGGGCTGCCATCGAGG
	S-5' RACE	GTCAGCCTTGTTCCTTCCTGCCTC
RNA1 clone	TR11768-F1	GGCATGTGCTATCTGCTGGC
	TR11768-R1	TTCCTGACTTGCACTAACCCATC
	TR11768-F2	CTGCAATGTTCCAAGCCATCC
	TR11768-R2	CATGGCTATGACATAGCACATCG
RNA2 clone	2403-1353F	CACTCTGGAGGATGGAAGGCTTCTAG
	2403-2090R	GATGCTAGGTGGAGAAAGGGATCTTC
	5'-1374-F	GGAAGTCTTCCTTCATCACAGG
	5'-1374-R	CCACAACACAACACAAAGTCCC
	5'-2403-F	CCAATGAAGAAGGAGGAAGG
	5'-2403-R	ATGACTTCTCAGTACGACATTGC
RNA3 clone	N-61F	GGGACTTTGTGTGTTCTTAGCTGC
	N-981R	CGAAGTCCATCTCTCAGGATGAGTT
	N-1117R	ATGGCTTCCGCAGAGTCTGTG
	N-607F	CAGTGTAGAGCCAGAGGAGGGTC
Adapter primer	PC2	CCGAATTCCCGGGATCC
	PC3-T7 loop	GGATCCCGGGAATTCGGTAATACGACTCACTATATTT TTATAGTGAGTCGTATTA
Primers used for VmNSRV1 RT-PCR detection		

RNA1	L-5'-F	GATGACCAAACAAGCTGTGCAG
	L-5'-R	CCCTCATCACAAGGTGGCTC
RNA2	M-3'-F	GGTTCTCCATGTCATGGTTGTAGTC
	M-3'-R	GATCTGGAACCAGATCAGAGCTGAA
RNA3	S-5'-F	CAGCTAAGAACACACAAAGTC
	S-5'-R	CCAACCTTCATCTCATACTTC
Terminal universal primers	VmNSRV1-U-R	CACAAAGWCCCCCTYASMHMTWACR
Primers used for transient expression		
in *N. benthamiana*		
pBIN41-eGFP	pBIN41-eGFP-F	GCCCAAGCTTCGACTCTAGAGGATCCATGGTGAGC AAGGGCGAGGAGC
	pBIN41-eGFP-R	CGAATTCGAGCTCCCCGGGGGATCCTTACTTGTACA GCTCGTCCATGC
pBIN41-MP-L-eGFP	pBIN41-MP-L-eGFP-F	GCCCAAGCTTCGACTCTAGAATGACTTCTCAGTACG ACATTGC
	pBIN41-MP-L-eGFP-R	GCTCCTCGCCCTTGCTCACCATATTGAAAACATAAA CATCCTTTGTGT
pBIN41-N-eGFP	pBIN41-N-eGFP-F	GCCCAAGCTTCGACTCTAGAATGGCTTCCGCAGAGT CTGTG
	pBIN41-N-eGFP-R	GCTCCTCGCCCTTGCTCACCATGAAGGGGTTAAGGC CCTCGA
pBI121-MP-L	pBI121-MP-L-F	CACGGGGGACTCTAGAGGATCCATGACTTCTCAGTA CGACATTG
	pBI121-MP-L-R	TCACCATGGTACCCGGGGATCCATTGAAAACATAAA CATCCTTTGTGT
pBI121-N	pBI121-N-F	CACGGGGGACTCTAGAGGATCCATGGCTTCCGCAG AGTCTGTGTAT
	pBI121-N-R	TCACCATGGTACCCGGGGATCCGAAGGGGTTAAGG CCCTCGA
pBI121-TMV-30K	pBI121-30K-F	CACGGGGGACTCTAGAGGATCCATGGCTCTAGTTGT TAAAG
	pBI121-30K- R	TCACCATGGTACCCGGGGATCCAAACGAATCCGATT CGGCGACAG
Primers used for transient expression		
in fungus		

pCPX-eGFP/mCherry	pCPX-eGFP/mCherry-F	TTTTAGGTACGCGGCCGCAAGCTTACCATGGTGAG
	pCPX-eGFP/mCherry-R	GACGAGCTGTACAAGTAAGCATGCTTGACCTGATCTCCCA
pCPX-N-mCherry	pCPX-N-mCherry-F	TTTTAGGTACGCGGCCGCACCATGGCTTCCGCAGAGTCTG
	pCPX-N-mCherry-R	CTCACCATGGTGTTAACAAGCTTGAAGGGGTTAAGGCCCTCG
pCPX-MP-L-mCherry	pCPX-MP-L-mCherry-F	TTTTAGGTACGCGGCCGCACCATGACTTCTCAGTACGACATTG
	pCPX-MP-L-mCherry-R	CTCACCATGGTGTTAACAAGCTTATTGAAAACATAAACATCCTTTGTGT
pCPX-KEX-eGFP	pCPX-KEX-eGFP-F	TTTTAGGTACGCGGCCGCACCATGAAGATCACGGCCCT
	pCPX-KEX-eGFP-R	CTCACCATGGTGTTAACAAGCTTGTTAACACCATGGTGAG
pCPX-PER4-eGFP	pCPX-PER4-eGFP-F	TTTTAGGTACGCGGCCGCACCATGGCGGCGTCTCTACAG
	pCPX-PER4-eGFP-R	CTCACCATGGTGTTAACAAGCTTTTTGTTATGCCAGACAAA
pCPX-Erg28-eGFP	pCPX-Erg28-eGFP-F	TTTTAGGTACGCGGCCGCACCATGGACCACCTATACAACTTGCT
	pCPX-Erg28-eGFP-R	CTCACCATGGTGTTAACAAGCTTAGCCTTCACATAGTGGCTGTATTG
pCPX-SecE-eGFP	pCPX-SecE-eGFP-F	TTTTAGGTACGCGGCCGCACCATGGCCGACCAAGTGTCAG
	pCPX-SecE-eGFP-R	CTCACCATGGTGTTAACAAGCTTTGCGCCGCCGACGAGGATAT
Primers used for bacterial expression		
pMAL-c2x-MBP-N	c2x-N-F	TCAGAATTCGGATCCTCTAGAATGGCTTCCGCAGAGTCTGTGTATG
	c2x-N-R	ACGACGGCCAGTGCCAAGCTTCTAGAAGGGGTTAAGGCCCTCGATG
Primers used for Northern blot probes		
RNA1 detection	L5'-F	TAGCACAATCTCAAATGTCTTTCCG
	L5'-R	GAAGCCAGATGCCATGTTGTCA
RNA2 detection	M5'-F	GACCATCCACACCTCTCTGATCTTC

	M5'-R	GACCATGCAGATGTTGTGTTCACAT
RNA3 detection	S-5'-F	CAGCTAAGAACACACAAAGTC
	S-5'-R	CCAACCTTCATCTCATACTTC
Primers used for *V. mali*		
	VmF	GAGTACTCCCTCCCGCTCCG
	VmR	TTAATTAAGGGGCGGCCTCA
Primers used for *M. domestica*		
	Apple-18s-F	CTCTGCCCGTTGCTCTGATG
	Apple-18s-R	CTGCTGCCTTCCTTGGATGTG

Table S2. List of plasmid constructs generated in this study.

Construct	Insertion (region)	Plasmid	Restriction sites	Expressed in organism
MBP-N	VmNSRV1-N	pMAL-c2x-MBP	*Xba*I and *Hind*III	*E. coli*
eGFP	eGFP	pBIN41	*BamH*I	Plant
N-eGFP	N	pBIN41-eGFP	*Xba*I	Plant
MP-L-eGFP	MP-L	pBIN41-eGFP	*Xba*I	Plant
N-mCherry	N	pBI121-mCherry	*BamH*I	Plant
MP-L-mCherry	MP-L	pBI121-mCherry	*BamH*I	Plant
TMV-30K-mCherry	TMV-30K	pBI121-mCherry	*BamH*I	Plant
eGFP	eGFP	pCPXHY2	*Not*I and *Sph*I	Fungus
Erg28- eGFP	Erg28	pCPXHY2-eGFP	*Not*I and *Hind*III	Fungus
SecE-eGFP	SecE	pCPXHY2-eGFP	*Not*I and *Hind*III	Fungus
KEX-eGFP	KEX	pCPXHY2-eGFP	*Not*I and *Hind*III	Fungus
PER4-eGFP	PER4	pCPXHY2-eGFP	*Not*I and *Hind*III	Fungus
mCherry	mCherry	pCPXHY2	*Not*I and *Sph*I	Fungus
N-mCherry	N	pCPXHY2-mCherry	*Not*I and *Hind*III	Fungus
MP-L-mCherry	MP-L	pCPXHY2-mCherry	*Not*I and *Hind*III	Fungus

SI Materials and methods

Phylogenetic analysis

Maximum likelihood (1) tree construction was performed as described previously (2). For the amino acid alignment of the large protein L (polymerase), the MAFFT version 7 online service (https://mafft.cbrc.jp/alignment/server/) (3) was used with default parameters. Poorly aligned regions in the alignment were removed using TrimAI software version 1.3 (strict plus option) in the Phylemon 2.0 online platform (http://phylemon2.bioinfo.cipf.es) (4). The ML tree was constructed using the IQ-TREE online program (http://iqtree.cibiv.univie.ac.at) (5). The best-fit model (LG+F+I+G4) was selected by ModelFinder in IQ-TREE (6). The branch numbers indicate SH-aLRT support (%)/ultrafast bootstrap support (%); only values >80% are shown (7). Established (selected) members of the family *Phenuiviridae* (8) and the unassigned phenuivirids, which may belong to novel genera, were used for tree construction. The two leishbuvirids were used as the distant outgroups in the tree. The phylogenetic trees were then visualized using FigTree software version 1.3.1 (nucleobytes.com/enzymex/index.html).

Fungal and viral inoculations

The mechanical inoculation of viruses on the leaves of plants was carried out as described previously (9). VmNSRV1 purified fractions isolated from a virus-infected strain (QX-4-5) were rubbed on carborundum-dusted leaves of *N. benthamiana* and *M. domestica.* Virus infection in the leaves was detected by RT-PCR at 14 days after inoculation. The virus-infected fungus that grows on PDA was cut into a small piece (roughly 6 mm^2) and inoculated on the leaves of *M. domestica*. After inoculation, at 14 days, the total RNA of the systemic leaves was extracted, and the virus was detected by RT-PCR.

To investigate the acquisition of VmNSRV1 by *V. mali*, a virus-free *V. mali* strain QX-4-5 (a single-spore isogenic strain) was inoculated on the leaves of *M. domestica* already infected with VmNSRV1, and fungal colonization was allowed for 1 week. Fungi were re-isolated from the fungal lesions on leaves as described previously (10). Re-isolated fungi were identified using the sequencing of ITS regions amplified by PCR, and VmNSRV1 infection was detected by RT-PCR.

Pathogenicity assays

Pathogenicity assays on *V. mali* (QX-4-5) strains using apple fruits and twigs were carried out as described previously (11). The fungal colonies were cultured on PDA medium at 25 °C for 3 days. The area of lesions on apple fruits and the length of lesions on the twigs induced by fungal growth were measured as indicators of virulence (12). To test the effectiveness of VmNSRV1 in reducing fungal

pathogenicity, two experiments were carried out. In the first experiment, the fungal mycelial plug (~5 mm × ~5 mm) of a virus-free strain was inoculated on 2-year-old apple twigs and leaves obtained from an apple orchard at Northwest A&F University, China. After 2 days of inoculation, the mycelial plugs of virus-infected strains were placed on two points where fungal colonization of the virus-free strain had been established (2 cm above and below). In the second experiment, the purified virus fractions (50 μL) were applied directly three times (on three consecutive days) to apple twigs that had been inoculated with a virus-free strain. For the negative control inoculation, 0.05 M phosphate-buffered saline (PBS) was used. Ten days after inoculation, lesion size was measured, *V. mali* strains were re-isolated, and the virus was detected by RT-PCR. Each inoculation was repeated three times. The surfaces of the fruits, leaves, and twigs were washed with sterile water and wiped with 75% ethanol before inoculation. The inoculation materials were placed in a sterile container in a humid environment.

Prokaryotic protein expression and antibody preparation

The coding sequence of the VmNSRV1 N gene was inserted into the pMAL-c2x bacterial expression plasmid (13), resulting in an MBP (maltose binding protein)-N fusion construct. The recombinant plasmid was transformed into BL21 Star (DE3) Chemically Competent Cells (Tsingke, China). MBP-N was expressed and examined by SDS-PAGE. The N protein was purified using the Dextrin Beads 6FF kit (Smart-Lifesciences, China). The protein was dissolved in 1 mL buffer (20 mM Tris-HCl, 1 mM EDTA, and 10 mM maltose, pH 7.4) and dialyzed with 0.9% NaCl in Regenerated Cellulose Dialysis Membranes (34 mm, 3.5 kDa, Beyotime, China), then concentrated with solid sucrose and subcutaneously emulsified with Freund's adjuvant (incomplete, Sigma-Aldrich, USA). Antigen (1 mg/mL) was injected into New Zealand white rabbits. N protein antiserum was prepared by Shengong Biotech Co. Ltd. (Shanghai, China).

Western blot and northern blot analyses

Western blot analysis was carried out as described previously (14). VmNSRV1 N was detected using an anti-VmNSRV1 N polyclonal antibody (1:5,000) and a secondary polyclonal antibody (1:10,000; HRP-conjugated anti-rabbit IgG, Abcam, UK). The eGFP was detected using a GFP mouse polyclonal antibody (1:5,000; SAB, USA) and a secondary polyclonal antibody (1:10,000; HRP-conjugated anti-mouse IgG, Abcam). The protein bands were developed using a western blot ECL Substrate kit (Bio-Rad, USA) and observed with ChemiDoc Imaging Systems (CLiNX, China).

Northern blot analysis was carried out as previously described (14). Digoxigenin-labeled DNA probes were prepared by PCR with the primers listed in *SI Appendix*, Table S1.

Virus particle purification

The method used for virus purification was generally based on a previously described purification method (15). Fungal strains were cultured in 400 mL potato dextrose broth (PDB) for 5 days at 25 °C in the dark. The mycelia were homogenized in 6 mL of 0.05 M PBS (pH 7.4). The suspensions were centrifuged at 10,000 rpm for 10 min at 4 °C twice. The supernatant was transferred to a 13.2 mL ultra-clear tube (Beckman), and then 3 mL of 20% sucrose solution was slowly added to the bottom of the solution, followed by centrifugation at 21,000 rpm for 2 h at 4 °C in a Beckman SW41Ti rotor. The pellet was suspended with 4 mL 0.05 M PBS, applied on top of a 10–40% sucrose density gradient in 0.05 M Na_2CO_3 buffer, and subjected to centrifugation at 20,000 rpm for 2 h at 4 °C in a Beckman SW41Ti rotor. After centrifugation, the gradient was equally separated into six fractions from top to bottom, diluted in 0.05 M PBS buffer, and centrifuged at 25,000 rpm for 2 h at 4 °C. The pellet was suspended in 100 μL of 0.05 M PBS.

Lipid droplet fractionation

Lipid droplet (LD) detection of the virus-infected and virus-free strains with Erg28-eGFP was based on the virus particle purification method, except that during the first step after homogenization of the mycelia using 0.05 M PBS buffer, the suspensions were centrifuged at 6,000 rpm for 10 min at 4 °C twice. The 10–40% sucrose gradient in 0.05 M Na_2CO_3 was also used to separate different densities of LDs. The proteins of each fraction were collected and examined using Western blot analysis.

Transmission electron microscopy observation

A carbon-coated copper/rhodium grid (200 mesh, EMCN, China) was floated for 30 min on a small drop (20 μL) of purified virus preparation and rinsed with 50 μL of double-distilled water twice. Negative staining was performed with 20 μL of 2% w/v uranyl acetate solution (HEAD, China) for 3 min. The virus-infected strain and virus-free strain s of the *V. mali* (QX-4-5) strain were cultured on PDA plates layered with cellophane for 3 days. Mycelia were placed in 1-hexadecane solution (Sigma-Aldrich, USA) and sandwiched between two flat aluminum plates. Samples were frozen rapidly using an EM ICE high-pressure freezing machine (Leica, Germany) as described previously (16). Ultrathin sections were cut from the embedded tissues with an ultramicrotome (Leica, Germany) and then stained with uranyl acetate and lead citrate. The specimens were examined under a transmission electron microscope (Hitachi JEM-

1230, Japan). The number of LDs in 10 μm^2 region of ultrathin section in virus-free and VmNSRV1-infected *V. mali* hypha was quantified. The diameter of LDs was measured by ImageJ software (1.54t Fiji).

SI Reference

1. A. Shamloul, A. Hadidi, S. Zhu, R. Singh, B. J. C. J. o. P. P. Sagredo, Sensitive detection of potato spindle tuber viroid using RT-PCR and identification of a viroid variant naturally infecting pepino plants. *Can. J. Plant Pathol.* **19**, 89-96 (1997).
2. H. Kondo *et al*., Discovery and Genome Characterization of a Closterovirus from Wheat Plants with Yellowing Leaf Symptoms in Japan. *Pathogens* **12**, 358 (2023).
3. K. Katoh, D. M. Standley, MAFFT multiple sequence alignment software version 7: improvements in performance and usability. *Mol. Biol. Evol*. **30**, 772-780 (2013).
4. R. Sanchez *et al*., Phylemon 2.0: a suite of web-tools for molecular evolution, phylogenetics, phylogenomics and hypotheses testing. *Nucleic Acids Res*. **39**, W470-W474 (2011).
5. J. Trifinopoulos, L.-T. Nguyen, A. von Haeseler, B. Q. Minh, W-IQ-TREE: a fast online phylogenetic tool for maximum likelihood analysis. *Nucleic Acids Res*. **44**, W232-W235 (2016).
6. S. Kalyaanamoorthy, B. Q. Minh, T. K. Wong, A. Von Haeseler, L. S. Jermiin, ModelFinder: fast model selection for accurate phylogenetic estimates. *Nat. Methods*. **14**, 587-589 (2017).
7. D. T. Hoang, O. Chernomor, A. Von Haeseler, B. Q. Minh, L. S. Vinh, UFBoot2: improving the ultrafast bootstrap approximation. *Mol. Biol. Evol*. **35**, 518-522 (2018).
8. T. Sasaya *et al*., ICTV Virus Taxonomy Profile: *Phenuiviridae* 2023. *J. Gen. Virol*. **104**, 001893 (2023).
9. R. Bian *et al*., Facilitative and synergistic interactions between fungal and plant viruses. *Proc. Natl. Acad. Sci. U. S. A*. **117**, 3779-3788 (2020).
10. I. B. Andika *et al*., Phytopathogenic fungus hosts a plant virus: A naturally occurring cross-kingdom viral infection. *Proc. Natl. Acad. Sci. U. S. A*. **114**, 12267-12272 (2017).
11. S. Yang *et al*., Infection of Two Heterologous Mycoviruses Reduces the Virulence of *Valsa mali*, a Fungal Agent of Apple Valsa Canker Disease. *Front Microbiol*. **12**, 659210 (2021).
12. B. I. Hillman, S. Supyani, H. Kondo, N. Suzuki, A Reovirus of the Fungus *Cryphonectria parasitica* That Is Infectious as Particles and Related to the *Coltivirus* Genus of Animal Pathogens. *J. Virol*. **78**, 892-898 (2004).
13. I. H. Walker, P.-c. Hsieh, P. D. Riggs, Mutations in maltose-binding protein that alter affinity and solubility properties. *Appl. Microbiol. Biotechnol*. **88**, 187-197 (2010).
14. L. Sun, N. Suzuki, Intragenic rearrangements of a mycoreovirus induced by the multifunctional protein p29 encoded by the prototypic hypovirus CHV1-EP713. *RNA* **14**, 2557-2571 (2008).
15. Alioto *et al*., Improved detection of citrus psorosis virus using polyclonal and monoclonal antibodies. *Plant Pathol*. **48**, 735-741 (1999).
16. M. Yue *et al*., Coronaviral ORF6 protein mediates inter–organelle contacts and modulates host cell lipid flux for virus production. *EMBO J*. **42**, e112542 (2023).